DOI: 10.1002/ejic.201100790

# Magnetic and Sorption Properties of Supramolecular Systems Based on Pentanuclear Copper(II) 12-Metallacrown-4 Complexes and Isomeric Phthalates: Structural Modeling of the Different Stages of Alcohol Sorption

**Anna V. Pavlishchuk,[a] Sergey V. Kolotilov,*[b] Matthias Zeller,[c] Oleksiy V. Shvets,[b] Igor O. Fritsky,[a] Samuel E. Lofland,[d] Anthony W. Addison,*[e] and Allen D. Hunter[c]**

**Keywords:** Metallacrown compounds / Copper / Sorption / Magnetic properties

Metathesis of the perchlorate anions in $[Cu_5(ahpha)_4](ClO_4)_2 \cdot 4H_2O$, where $ahpha^{2-}$ is the dianion of 3-amino-3-hydroximinopropane hydroxamic acid, with *m*- and *p*-phthalates resulted in formation of $[Cu_5(ahpha)_4(m\text{-}C_8H_4O_4)(H_2O)] \cdot 9H_2O$ (**1**), $[Cu_5(ahpha)_4(m\text{-}C_8H_4O_4)(H_2O)] \cdot 2MeOH \cdot DMF$ (**1a**) and $[Cu_5(ahpha)_4(p\text{-}C_8H_4O_4)(H_2O)_2]_2 \cdot 14H_2O$ (**2**). Molecules in the structures of **1**, **1a** and **2** are held together by noncovalent interactions, and the lattices contain voids filled with water molecules. Compounds **1** and **1a** differ in the mode of *m*-phthalate coordination, solvent type, and crystal lattice content. Desolvated **1** and **2** sorb gaseous MeOH and EtOH. Whereas the MeOH sorption capacity was very similar for **1** and **2** (about 0.14 $cm^3/g$ at $PP_S^{-1} = 0.9$, where $P$ is the current methanol pressure and $P_S$ the saturation vapor pressure of methanol at 293 K), the capacity of **2** to sorb EtOH was about 1.5 times as high as that of **1**. To a certain extent, the structures of **1** and **1a** can be considered as models of compounds that can form at different stages during alcohol sorption by desolvated **1**. The $\chi_M T$ vs. $T$ data for **1** and **2** could be fitted with a model based on the Hamiltonian $H(Cu^{II}_5) = -2J_1(S_1 \cdot S_2 + S_1 \cdot S_3 + S_1 \cdot S_4 + S_1 \cdot S_5) - 2J_2(S_2 \cdot S_5 + S_2 \cdot S_3 + S_3 \cdot S_4 + S_4 \cdot S_5)$, where $S_1$ represents the spins of the central $Cu^{II}$ ions and $S_2$–$S_4$ correspond to the spins of the peripheral $Cu^{II}$ ions. The best fits corresponded to $J_1 = -129(3)\ cm^{-1}$, $J_2 = -66(1)\ cm^{-1}$ and $zJ' = -2.5(2)\ cm^{-1}$ at $g_{Cu} = 2.12(1)$ for **1**, and $J_1 = -163(3)\ cm^{-1}$, $J_2 = -78(1)\ cm^{-1}$ and $zJ' = -1.5(1)\ cm^{-1}$ at $g_{Cu} = 2.05(1)$ for **2**.

## Introduction

Interest in coordination compounds that possess the ability to sorb various substrates is stimulated by the possibilities for their application for selective sorption,[1] the separation of different compounds,[2] and catalysis.[3] Porous coordination polymers as sorbent lattices can contain paramagnetic metal ions that may lead to the polymer displaying nontrivial magnetic properties. In contrast to diamagnetic sorbents, such as porous carbons or zeolites, the interaction of coordination polymers with sorbed substrates may cause structural rearrangements and hence changes in the physical properties e.g. magnetic properties of the polymer.[4] Such compounds may be considered as a basis for the generation of chemical sensors,[5] as well as magnetic materials with tunable properties, which makes studies of the interaction of coordination polymers with various substrates an important field in contemporary coordination chemistry and material science.[6]

Among the variety of compounds called "porous coordination polymers", two types can be distinguished: sorbents with rigid structures[7] and "breathing polymers" with flexible structures.[8] In the latter case, sorption and desorption of certain substrates induce changes in the crystal structure, which may be associated with changes in the solvent accessible void volume.[9,10] It has also been shown that compounds built from discrete units (i.e. not polymers), can sorb small molecules.[11,12] Such sorption is usually associated with specific host-guest interactions between the sorbate and structural elements of the sorbent.[13] It is important to understand the nature of such interactions as well as any attendant structural changes that can occur during

[a] Department of Chemistry, National Taras Shevchenko University
Volodymyrska str. 62, Kiev 01033,Ukraine
Fax: +380-44-239-33-93
E-mail: annpavlis@ukr.net, ifritsky@univ.kiev.ua
[b] L.V. Pisarzhevskii Institute of Physical Chemistry of the National Academy of Sciences of the Ukraine
Prospect Nauki 31, Kiev 03028, Ukraine
Fax: +380-44-525-62-16
E-mail: svk001@mail.ru
[c] STaRBURSTT CyberInstrumentation Consortium, Youngstown State University, Department of Chemistry,
One University Plaza, Youngstown Ohio 44555-3663, USA
Fax: +1-330-941-15-79
E-mail: mzeller@ysu.edu
adhunter@ysu.edu
[d] Department of Physics and Astronomy, Rowan University, Glassboro, New Jersey 08028, USA
Fax: +1-856-256-43-82
E-mail: lofland@rowan.edu
[e] Department of Chemistry, Drexel University, Philadelphia, PA 19104-2816, USA
Fax: +1-215-895-12-65
E-mail: AddisonA@drexel.edu

Supporting information for this article is available on the WWW under http://dx.doi.org/10.1002/ejic.201100790.

 WILEY ONLINE LIBRARY © 2011 Wiley-VCH Verlag GmbH & Co. KGaA, Weinheim 

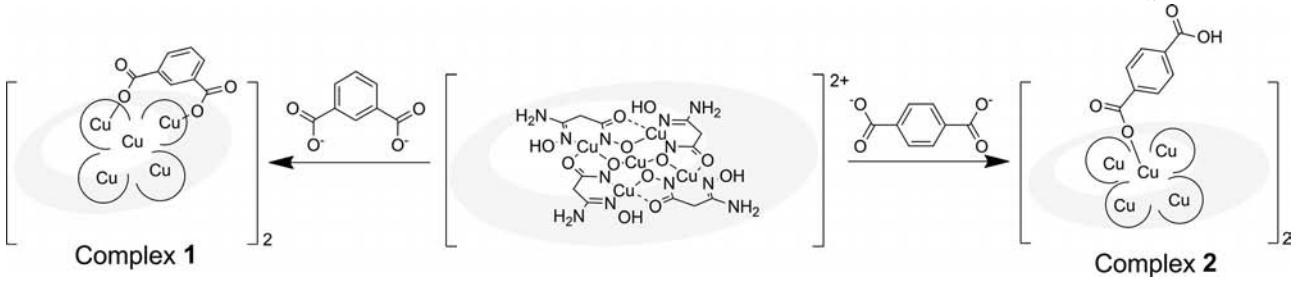


Figure 1. Scheme showing the formation of complexes **1** and **2** from $[Cu_5(ahpha)_4]^{2+}$. Note that for compound **2** only the asymmetric half of the dimer is shown.

such sorption and desorption processes. In addition, the development of new systems based on polynuclear "building blocks" and that are capable of interacting with small molecules is important for obtaining compounds with predetermined magnetic and spectral properties, which may be governed by the properties of the starting polynuclear units.

Metallacrowns have been attracting attention for several reasons, which include their intramolecular magnetic exchange interactions,[14,15] bioactivity[16] and their ability to exhibit selective recognition of cations and anions.[17] Due to the presence of coordination positions on the metal ions that are vacant or occupied by readily displaceable ligands, metallacrowns can be linked by appropriate bridging ligands, such as carboxylates, to give novel supramolecular assemblies.[18] Such systems, along with the intrinsic properties of the constituent metallacrowns, may possess properties that result from the specific crystal packing, such as the capacity to sorb certain substrates.[12] Sorption may be achieved by filling of the voids in crystal structures, as well as by substrate-induced rearrangement of the crystal lattice. A few examples of compounds based on metallacrown units with large void volumes have been reported, however information on the sorption properties of such systems is scarce.[12,19]

The aim of this research was to study the possibility for the generation of porous structures by linking pentanuclear metallacrowns with dicarboxylates, to examine the capacity of the resulting compounds for the sorption of various substrates, and to obtain information about possible changes that occur in the crystal structure of the sorbent due to its interaction with sorbates. An additional aim of this study was to see to what extent structural deformation of the pentanuclear cation, induced by coordination of an additional ligands, can change the magnetic coupling ($J$ values) associated with the intramolecular $Cu^{II}\cdots Cu^{II}$ interactions. In order to have more data to enable comparison of the $J$ values, we used the well characterized cationic pentacopper metallacrown $[Cu_5(ahpha)_4]^{2+}$, which has previously been reported, as a constituent of several different compounds.[12,20] $[Cu_5(ahpha)_4]^{2+}$ has vacant positions in the coordination spheres of the $Cu^{2+}$ ions, it has a planar structure and is stable in solution, which makes it a suitable "building block" for assembling high nuclearity systems and supramolecular architectures.

In this paper we report the synthesis, XRD determined structures, alcohol sorption and magnetic properties of three coordination compounds, **1**, **1a** and **2**, which were obtained by the combination of the cationic metallacrown $[Cu_5(ahpha)_4]^{2+}$ with anions of the isomeric *m*- and *p*-phthalates 1,3- and 1,4-benzenedicarboxylate (Figure 1).

## Results and Discussion

### Synthesis

Formation of **1** vs. **1a**, which differ in the coordination mode of *m*-phthalate and in solvent composition (vide infra), was governed by the solvent used in the reaction ($DMF/H_2O$ and DMF-methanol mixtures, respectively). Coordination of *m*- or *p*-phthalate dianions to the $Cu^{II}$ ions in $[Cu_5(ahpha)_4]^{2+}$ results in anion metathesis that leads to the formation of neutral complexes **1**, **1a** and **2**, which contrast with the ionic starting compound. In addition, the reaction involves dimerization of the $[Cu_5(ahpha)_4]^{2+}$ units, which results in decanuclear compounds (Figure 1). Several complexes containing the cation $[Cu_5(ahpha)_4]^{2+}$ have previously been reported, such as the nitrate salt in which $Cu_5$ cations are stacked in a 1D polymer,[20] and the adduct with $Cr(C_2O_4)_3^{3-}$ that contains a trimeric $Cu_{15}$ core.[12] It may be noted that there is a connection between the degree of pentacopper block oligomerization and the charge of counter –anions: 1D chains have anions with a –1 charge, dimers or stacks of weakly bonded pentanuclear cations have anions with a –2 charge, and trimers have anions with a –3 charge. The perchlorate salt of $[Cu_5(ahpha)_4]^{2+}$ also follows this trend (see Supporting Information). However, formation of a given type of structure is definitely directed not only by the anion's charge, but also by its coordination ability, as well as the lattice energy of the resulting compound.

### XRD Determined Structures

Crystal data, data collection parameters and structure refinement details for complexes **1**, **1a** and **2** are given in Table 2 (see Exp. Sect.).

 © 2011 Wiley-VCH Verlag GmbH & Co. KGaA, Weinheim 

**Complex 1 $[Cu_5(ahpha)_4(m\text{-}C_8H_4O_4)(H_2O)]\cdot 9H_2O$.** The crystal structure of complex **1** consists of neutral centrosymmetric stacks of weakly bonded (vide infra) pentanuclear units of $[Cu_5(ahpha)_4(m\text{-}C_8H_4O_4)(H_2O)]_2$ and 18 nonbonded water molecules per $[Cu_5]_2$ unit. Two *m*-phthalates are bonded to the "external" sides of the $[Cu_5]_2$ unit, each *m*-phthalate dianion is coordinated in a monodentate fashion to two peripheral $Cu^{II}$ ions through two oxygen atoms from two deprotonated carboxylic groups (Figure 2). Individual neighboring $[Cu_5(ahpha)_4(m\text{-}C_8H_4O_4)]$ units are related by an inversion center and are linked by rather long [2.894(5) Å] out-of-plane hydroxamate Cu3–O10′ contacts, which may be considered as very long Cu–O axial bonds, although the O10′ atoms may simply be residing in an electrostatic energy minima that is adjacent to the neighboring $Cu_5$ unit (Figure S1).

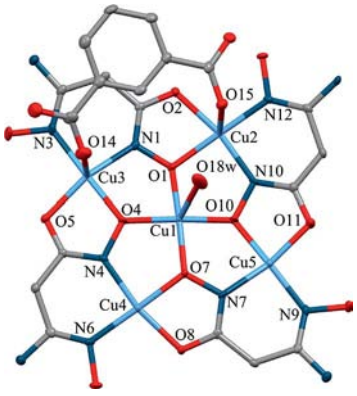


Figure 2. The structure of a $[Cu_5(ahpha)_4(m\text{-}C_8H_4O_4)(H_2O)]$ unit that is present in **1**. Two such units are stacked, and exhibit long Cu3–O10′ [2.894(5) Å] contacts. Hydrogen atoms are omitted for clarity. Thermal ellipsoids are drawn at the 50% probability level.

Each pentanuclear cation $[Cu_5(ahpha)_4]^{2+}$ consists of four peripheral $Cu^{II}$ ions, located in the $Cu_4$ metallacrown ring of the $[Cu_5(ahpha)_4]^{2+}$ unit, and one central $Cu^{II}$ ion. The cavity in which this central copper ion sits is formed by four hydroxamate oxygen atoms. Each of the four deprotonated $ahpha^{2-}$ ligands binds to three $Cu^{II}$ ions – two peripheral ions and one central ion. The peripheral $Cu^{II}$ ions have two oxygen donors (one from a carbonyl group, and the second from the deprotonated hydroxamate N-O group) and two nitrogen donors from two different oximate and hydroxamate N-O groups in the equatorial positions. While the $CuO_5$ chromophore containing the central $Cu^{II}$ ion, Cu1, is unequivocally square pyramidal ($\tau$ = 0.004),[21] the peripheral $Cu^{II}$ ions have slightly distorted square pyramidal $N_2O_3$ coordination environments [$\tau$(Cu2) = 0.18].[21] The axial positions of the Cu1 and Cu2 ions in **1** are occupied by a water molecule [Cu1–O18w, 2.468(5) Å] and a carboxyl oxygen atom, O15, from a *m*-phthalate ligand [Cu2–O15, 2.640(4) Å], respectively. Atom Cu3 is bound by an $N_2O_4$ donor set with elongated octahedral geometry. The axial positions of the Cu3 ion are occupied by a carboxyl oxygen atom, O14, from a *m*-phthalate ligand [Cu3–O14, 2.591(5) Å] and a hydroxamate oxygen atom, O10′, [Cu3–O10′, 2.894(5) Å] from a neighboring $Cu_5$ unit. The *m*-phthalate dianion is bound to two peripheral copper atoms (Cu2 and Cu3). Copper ions Cu4 and Cu5 exhibit distorted square planar geometry and are bound by $N_2O_2$ donor sets. In the case of Cu5 the square planar distortion is greater (the angle between the O11–Cu5–N9 and O10–Cu5–N7 planes is 12.6°) than for Cu4 (the O7–Cu4–N4 and O8–Cu4–N6 planes are twisted by 2.6° with respect to each other).[22]

All the equatorial Cu–O and Cu–N bond lengths lie within the range 1.885(3)–1.987(3) Å, while the bonds with the donor groups in the axial positions are longer, evidencing the Jahn–Teller distortion of the $Cu^{II}$ chromophores. Selected bond lengths and angles are presented in Table S1. The non-hydrogen atoms of the metallacrown fragment $[Cu_5(ahpha)_4]^{2+}$ in **1** are close to being coplanar: the deviation of the central copper ion, Cu1, from the plane defined by the peripheral copper ions Cu2, Cu3, Cu4, and Cu5 is 0.099(2) Å, while the largest deviation from this plane by the non-hydrogen atoms is 0.883(3) Å (for N11). The angle between the mean plane defined by the peripheral copper ions (Cu2–Cu3–Cu4–Cu5) and the *m*-phthalate's aromatic ring plane (C14–C15–C16–C17–C18–C19) is only 12.0(1)°.

π-Stacking between the aromatic rings of the *m*-phthalates [the separation between the parallel benzene ring mean planes is 3.279(4) Å] leads to the formation of pseudo-1D chains comprising $[Cu_5(ahpha)_4(m\text{-}C_8H_4O_4)(H_2O)]_2$ units (Figure 3). An extended system of hydrogen bonds [O8–H12B, 2.202(4) Å; O12–H5D, 2.225(3) Å; O14–H8D, 1.941(2) Å; O15–H11D, 2.035(4) Å] leads to packing of these 1D chains in the other two dimensions, so that comparatively large channels [16.5 × 6.1 $Å^2$] are formed in the crystal lattice that extend along the *a* axis (see Figure 3 and Figures S2 and S3 in the Supporting Information). These channels are filled with water molecules.

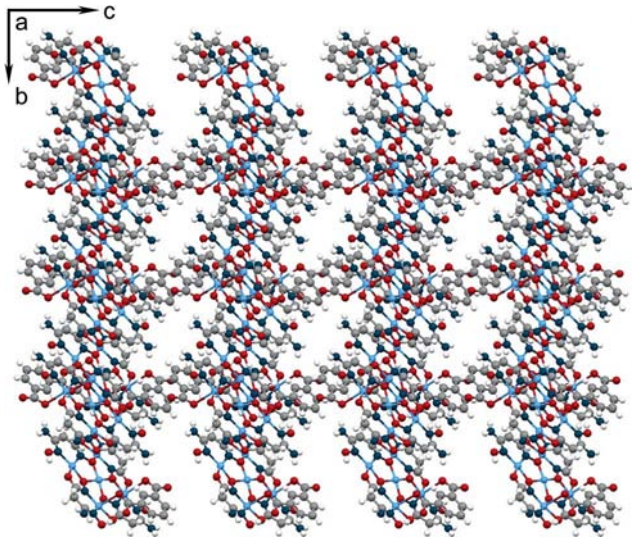


Figure 3. Fragment of the crystal structure of complex **1**, as viewed along the *a* axis. Solvent molecules (both coordinated and noncoordinated) are omitted for clarity.

 © 2011 Wiley-VCH Verlag GmbH & Co. KGaA, Weinheim 

PLATON[23] calculations (with a probe molecule that has a radius of 1.4 Å) indicate that removal of all coordinated and noncoordinated solvent molecules from the otherwise intact lattice would leave voids in **1** corresponding to 397 Å$^3$, which is 20.6% of the unit cell volume (as an upper limit).

**Complex 1a [$Cu_5$(ahpha)$_4$(*m*-$C_8H_4O_4$)($H_2O$)]·2MeOH·DMF.** The crystal structure of complex **1a** consists of neutral [$Cu_5$(ahpha)$_4$(*m*-$C_8H_4O_4$)($H_2O$)] and noncoordinated methanol and DMF molecules. The *m*-Phthalate dianion is coordinated to a peripheral Cu4 ion of the [$Cu_5$(ahpha)$_4$]$^{2+}$ cation through carboxylate oxygen O14 [Cu4–O14, 2.360(3) Å], the phthalate's other carboxylate group remains uncoordinated. The Cu containing molecules are arranged centrosymmetrically, with their phthalate groups positioned on the symmetry element, they also lie parallel but slipped with respect to each other, and interact weakly via long Cu5–O9′ contacts [2.988(3) Å] (Figure 4, S4 and S5).

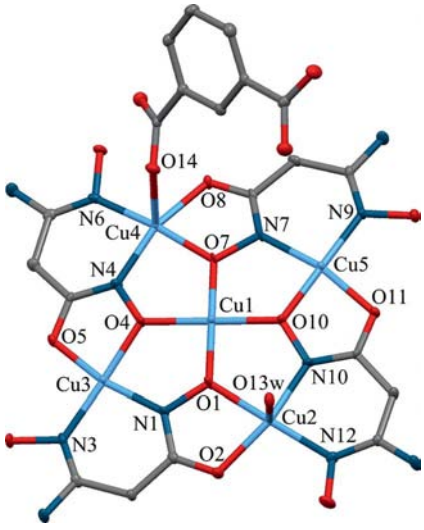


Figure 4. The structure of a [$Cu_5$(ahpha)$_4$(*m*-$C_8H_4O_4$)($H_2O$)] unit that is present in **1a**. Hydrogen atoms are omitted for clarity. Thermal ellipsoids are drawn at the 50% probability level.

The pentanuclear crowns in **1a** are arranged as stacks that lie along the *a* axis and are connected by multiple H-bonds. The arrangements of the [$Cu_5$(ahpha)$_4$]$^{2+}$ units in **1** and **1a** are further compared in the discussion of the sorption properties of these complexes (vide infra).

The structure of the metallacrown fragment, [$Cu_5$(ahpha)$_4$]$^{2+}$, in **1a** is generally similar to its structure in complex **1**, although slight differences in the coordination environments of the $Cu^{II}$ ions are observed, but only at the axial positions. Copper ions Cu1 and Cu3 in **1a** exhibit distorted square-planar geometries and are bound by $N_2O_2$ donor sets. The axial position of Cu2 is occupied by a water molecule [Cu2–O13w, 2.315(4) Å], while Cu4 binds, at its axial position, with carboxyl oxygen O14 from the *m*-phthalate ligand [Cu4–O14, 2.360(3) Å]. Copper ion Cu5 is bound by an $N_2O_3$ donor set and exhibits a distorted square pyramidal coordination geometry ($\tau$ = 0.15),[21] while the axial position of Cu5 is exposed to the hydroxamate atom, O9′, from a neighboring metallacrown unit. Selected bond lengths and angles are presented in Table S2.

PLATON[23] (as described above) estimates the total void volume in **1a** to be 1879 Å$^3$, which is 18.7% of the unit cell volume.

The cation [$Cu_5$(ahpha)$_4$]$^{2+}$ in **1a** is almost planar, the deviation of the central copper ion, Cu1, from the plane defined by the peripheral copper ions Cu2, Cu3, Cu4, and Cu5 is 0.127(4) Å, while the largest deviation from this plane is 0.480(3) Å (for N8). The angle between the plane defined by the peripheral copper ions (Cu2–Cu3–Cu4–Cu5) and the plane of the *m*-phthalate's aromatic ring (C14–C15–C16–C17–C18–C19) is 53.6(1)°, which is significantly larger than the corresponding angle in complex **1**.

The formation of an extended system of hydrogen bonds [O5–H13B, 1.903(5) Å; O14–H2C, 1.999(4) Å; O16–H8C, 1.996(4) Å; O16–H9, 1.813(5) Å; O17–H13A, 1.831(3) Å] leads to packing of decanuclear units in such a way that comparatively large voids [12.3 × 6.6 Å$^2$] are formed in the crystal lattice (Figure 5 and Figure S6). These voids can be represented as channels directed along the *b* axis. Similarly, as in the case of **1**, the voids in **1a** are filled with solvent molecules (DMF and methanol).

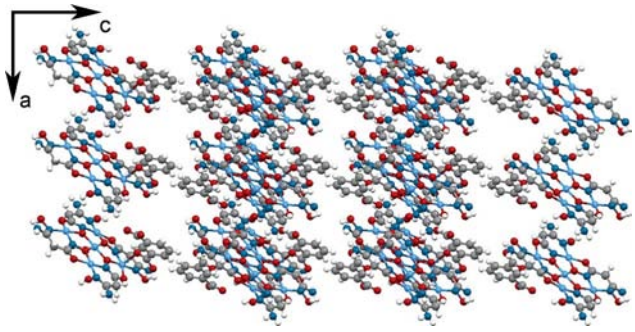


Figure 5. Fragment of the crystal structure of complex **1a**. [$Cu_5$(ahpha)$_4$(*m*-$C_8H_4O_4$)($H_2O$)] units are linked through long Cu5–O9′ [2.988(3) Å] contacts. Solvent molecules, both coordinated and noncoordinated, are omitted for visual clarity.

**Complex 2 [$Cu_5$(ahpha)$_4$(*p*-$C_8H_4O_4$)($H_2O$)$_2$]$_2$·14$H_2O$.** The crystal structure of complex **2** (Figure 6) consists of dimerized metallacrown [$Cu_5$(ahpha)$_4$]$^{2+}$ units with coordinated *p*-phthalate dianions in the ratio of 1:1, and water molecules that are both coordinated and captured in the voids.

The structure of the initial pentacopper metallacrown building block [$Cu_5$(ahpha)$_4$]$^{2+}$ is mainly retained within **2**, and several types of coordination polyhedra for the $Cu^{II}$ ions can be found within this complex. Copper ion Cu5 exhibits an essentially square planar geometry (the angle between the O10–Cu5–N7 and O11–Cu5–N9 planes is 12.7°) and is part of a $CuN_2O_2$ chromophore, while the other $Cu^{II}$ ions have slightly distorted square pyramidal geometries ($\tau$ ranges from 0.017 to 0.2) and are also components of $CuN_2O_3$ chromophores. The axial positions of Cu2 and Cu3 are occupied by oxygen atoms (O17w and O19w) of water molecules that are located on different sides of the [$Cu_5$(ahpha)$_4$]$^{2+}$ unit; atom O17w is on the side opposite to

 © 2011 Wiley-VCH Verlag GmbH & Co. KGaA, Weinheim 

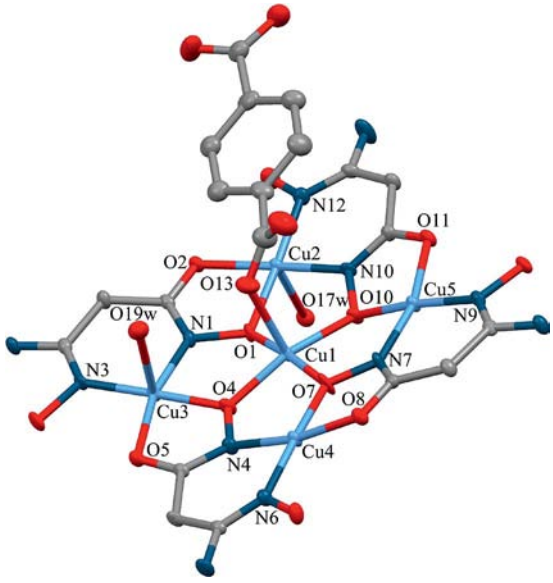


Figure 6. The structure of the $[Cu_5(ahpha)_4(p\text{-}C_8H_4O_4)(H_2O)_2]$ unit that is one half of a decanuclear $[Cu_5(ahpha)_4(p\text{-}C_8H_4O_4)(H_2O)_2]_2$ unit that is present in **2**. Two such units are dimerized through Cu4–O10′(oximate) bonds [2.677(4) Å]. Hydrogen atoms are omitted for clarity. Thermal ellipsoids are drawn at the 50% probability level.

the phthalate ligand, and O19w on the same side as the phthalate ligand (Figure S6). The phthalate dianion is bound in a monodentate manner to the central copper ion, Cu1 [Cu1–O13, 2.335(3) Å]. Formation of an axial Cu4–O10′(oximate) bond [2.677(4) Å] leads to face-to-face metallacrown dimerization, which also occurred in complexes **1** and **1a**. The metallacrown fragment in **2** is, in general, more distorted than the corresponding fragment in complex **1**. The deviation of the central copper ion Cu1 from the mean plane defined by the peripheral copper ions Cu2, Cu3, Cu4, and Cu5 is 0.139(3) Å, which is greater than the corresponding deviations in **1** [0.099(2) Å] and **1a** [0.127(4) Å]. Among the non-hydrogen atoms, the largest deviation from the Cu2–Cu3–Cu4–Cu5 plane is 0.696(4) Å (for C2), while the angle between the metallacrown plane (Cu2–Cu3–Cu4–Cu5) and the mean plane of the coordinated *p*-phthalate dianion (C14–C15–C16–C17–C18–C19) is 19.2(1)°. Table S3 contains selected bond lengths and angles for complex **2**.

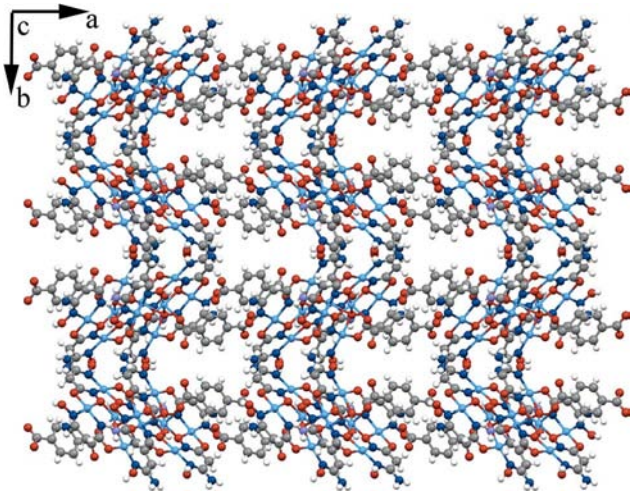


Figure 7. Fragment of the crystal structure of complex **2**, as viewed along the *c* axis. Solvent molecules (both coordinated and captured) are omitted for clarity.

The decanuclear $[Cu_5(ahpha)_4(p\text{-}C_8H_4O_4)(H_2O)_2]_2$ units are connected via an extended system of hydrogen bonds [H19B–O16, 1.799(2) Å] (Figures S7–S9), and are packed in such a way that $7 \times 4$ Å$^2$ channels are formed that lie along the *c* axis of the crystal lattice (Figure 7 and Figure S10 in the Supporting Information).

PLATON[23] estimates that the potential void volume for the crystal lattice of **2** is 441 Å$^3$, which is 11.8% of the cell volume.

## Magnetic Properties of Complexes 1 and 2

Magnetic susceptibility measurements over the temperature range 5–300 K were performed with polycrystalline samples of complexes **1** and **2** (Figure 8). The room temperature values of $\chi_M T$ for complexes **1** and **2** are 1.10 and 0.96 cm$^3$ K mol$^{-1}$, respectively, which are lower than the expected spin-only value (1.875 cm$^3$ K mol$^{-1}$) for five noninteracting $Cu^{2+}$ ($S$ = 1/2) ions with $g_{Cu}$ = 2.000. With decreasing temperature the $\chi_M T$ values fall, and at 5 K are to 0.37 and 0.36 cm$^3$ K mol$^{-1}$ for **1** and **2**, respectively, indicating that antiferromagnetic interactions dominate in both these compounds.

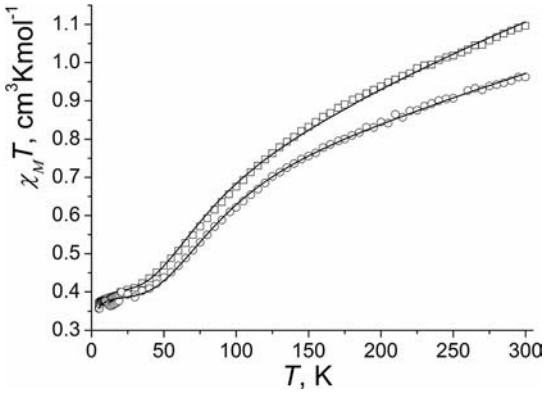


Figure 8. $\chi_M T$ vs. $T$ plots for complexes **1** (□) and **2** (○). The solid lines correspond to the curves calculated with parameters derived from the best fits to the data (Table S4).

The $\chi_M T$ vs. $T$ data were fitted with an expression[20] derived from the Hamiltonian, see Equation (1).

$$\mathcal{H}(Cu^{II}_5) = -2J_1(S_1 \cdot S_2 + S_1 \cdot S_3 + S_1 \cdot S_4 + S_1 \cdot S_5) - 2J_2(S_2 \cdot S_5 + S_2 \cdot S_3 + S_3 \cdot S_4 + S_4 \cdot S_5) \quad (1)$$

$J_1$ is the exchange integral between the central $Cu^{2+}$ ion and each of the four peripheral $Cu^{2+}$ ions, and $J_2$ is the exchange integral between each pair of adjacent peripheral $Cu^{2+}$ ions. Nonadjacent interactions between copper ions (like $S_2$–$S_3$ and $S_4$–$S_5$) were considered small enough to be

 © 2011 Wiley-VCH Verlag GmbH & Co. KGaA, Weinheim 

ignored. Potential intermolecular interactions were taken into account by application of the following molecular field model, see Equation (2).[24]

$$\chi_{MF}T = \frac{\chi_M T}{1 - \frac{zJ'\chi_M}{N_A g^2 \beta^2}} \quad (2)$$

The best fits for complexes **1** and **2** correspond to $J_1$ = –129(3) cm$^{-1}$, $J_2$ = –66(1) cm$^{-1}$ and $zJ'$ = –2.5(2) cm$^{-1}$ at $g_{Cu}$ = 2.12(1) for **1**, and $J_1$ = –163(3) cm$^{-1}$, $J_2$ = –78(1) cm$^{-1}$ and $zJ'$ = –1.5(1) cm$^{-1}$ at $g_{Cu}$ = 2.05(1) for **2**.[25]

The values obtained for the exchange parameters are very close to those reported previously for similar systems (Table 1). For all these compounds, $J_1$ lies in the range from –120 to –165 cm$^{-1}$, and $J_2$ varies between –65 and –85 cm$^{-1}$. We note that for the ahpha$^{2-}$ complexes (**1**–**4** in Table S4) the compounds with the highest deviations of the central $Cu^{2+}$ ion from the mean plane of the four peripheral $Cu^{2+}$ ions tend to have the highest absolute values for $J_1$. However, there is no obvious correlation between any structural parameter and the $J$ values.

Table 1. Magnetic properties of the complexes containing the pentanuclear cation $[Cu_5(ahpha)_4]^{2+}$. Data for an analogue is also included.

| | $g_{Cu}$ | $J_1$ [cm$^{-1}$] | $J_2$ [cm$^{-1}$] | $zJ'$ [cm$^{-1}$] | Deviation[e] | Ref. |
|---|---|---|---|---|---|---|
| **1** | 2.12(1) | –129(3) | –66(1) | –2.5(2) | 0.099 | this work |
| **2** | 2.05(1) | –163(3) | –78(1) | –1.5(1) | 0.139 | this work |
| **3**[a] | 2.066 (fixed) | –153(5) | –71(2) | –0.058(4) | 0.177[d] | [12] |
| **4**[b] | 2.066(3) | –119.9(7) | –79.0(4) | –0.69(7) | 0 | [20] |
| **5**[c] | 2.089(3) | –163(2) | –85.1(6) | –0.61(7) | 0.032 | [20] |

[a] Complex **3**: $\{[Cu_5(ahpha)_4]_3[Cr(C_2O_4)_3]_2 \cdot 4H_2O\} \cdot 8H_2O \cdot 1/3(DMF)$. [b] Complex **4**: $[Cu_5(ahpha)_4](NO_3)_2 \cdot 4H_2O$. [c] Complex **5**: $[Cu_5(hbha)_4](NO_3)_2 \cdot 8H_2O$, where $H_2$hbha = 3-(hydroximino)butanehydroxamic acid. [d] Average value for three $Cu_5$ blocks within one discrete molecule. [e] Deviation of the central $Cu^{2+}$ ion from the mean plane of the four peripheral $Cu^{2+}$ ions [Å].

## Thermogravimetric Analysis and Sorption Properties

Thermogravimetric (TG) data for complexes **1** and **2** did not show any weight losses corresponding to the elimination of all the water molecules from the structures until 220–230 °C. Plateaus could be distinguished in the TG curves at 130–180 °C for compound **1** (weight loss of 7–9.5%, corresponding to 3.5–5 $H_2O$ molecules remaining per $Cu_5$ unit) and 115–140 °C for compound **2** (weight loss of 6–8%, corresponding to 7–9.5 $H_2O$ molecules remaining per $Cu_{10}$ unit; Figures S11 and S12). Of the water molecules that are removed from **1** one is presumably the single coordinated $H_2O$ molecule (per $Cu_5$ unit), and of those removed from **2** four are the coordinated $H_2O$ molecules (per $Cu_{10}$ unit). The remaining water molecules that are removed are those situated within the lattice void spaces. Desolvation of **1** and **2** is also associated with at least partial collapse of their crystal structures, which is indicated by their powder X-ray diffraction patterns (decrease of intensity and shift of reflections to higher angles upon removal of the water molecules, Figures S13 and S14). Consequently, not all of the volume of the voids estimated by PLATON will be accessible to a sorbate after thermal desolvation of the lattices. Based on these TGA results, a sample activation temperature of 130 °C (at $10^{-2}$ Torr) was chosen for the sorption measurements, because these conditions seem to be sufficient for the elimination of the weakly bound lattice water, while avoiding the potential decomposition of the complexes that will occur at higher temperatures. Sorption isotherms were thus measured for compound **1** minus five water molecules (**1** – $5H_2O$) and compound **2** minus nine water molecules (**2** – $9H_2O$).

Compounds **1** and **2** showed only surface sorption of $N_2$ and $H_2$ at 77 K (their apparent surface areas, as estimated from the $N_2$ sorption isotherms, were less than 5 m$^2$/g). However, both compounds **1** and **2** sorbed substantial quantities of methanol and ethanol (Figures 9 and 10). Methanol uptake was almost zero at $PP_S^{-1} < 0.05$ for both compounds, but above this pressure the quantity of sorbed methanol increased sharply to ca. 0.01 cm$^3$/g (about 0.6 $CH_3OH$ molecule per $Cu_{10}$ unit, how these volumes were calculated is defined in the Exp. Section), which may be associated with structural rearrangements that result in an increase in the accessible volume – a situation that has been previously referred to as a "gates opening" phenomenon.[26,27] Such rearrangements may be caused by interactions of methanol molecules with the structural elements of the coordination compounds (vide supra).[9,11b] The second sharp increase in methanol binding was observed at a $PP_S^{-1}$ value of about 0.7, and the final sorption capacity was about 0.15 cm$^3$/g (ca. 9 $CH_3OH$ per $Cu_{10}$ unit, Figure S15) for compounds **1** and **2**. Over the full range of $PP_S^{-1}$ values the methanol sorption isotherm for **2** was higher than that for **1**. Except for this difference the methanol sorption and desorption curves for **1** and **2** were very similar. Hysteresis

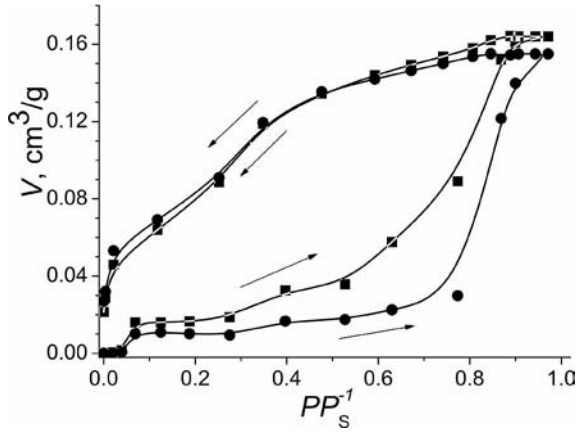


Figure 9. Isotherms recorded at 20 °C for methanol sorption and desorption by activated complexes **1** (●) and **2** (■).

 © 2011 Wiley-VCH Verlag GmbH & Co. KGaA, Weinheim 

was observed in the curves for both compounds, and some methanol could not be desorbed even at $10^{-2}$ Torr and room temperature, which may additionally evidence for a difference in the structures of the MeOH- and $H_2O$-solvated lattices. Though these isotherms are not typical of "classical sorption", they were reproducible with no substantial differences being present between data collected in several independently conducted experiments.

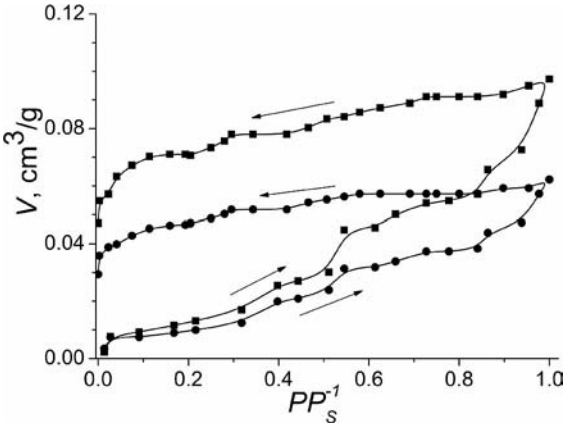


Figure 10. Isotherms recorded at 20 °C for ethanol sorption and desorption by activated complexes **1** (●) and **2** (■).

The features within the ethanol sorption/desorption isotherms for **1** and **2** (Figure 10) were generally similar to those in the methanol sorption/desorption curves. For both compounds, the ethanol sorption capacity was lower than in the case of methanol sorption, which is consistent with the larger size of the ethanol molecule compared to methanol. However in contrast to the methanol uptake, the total ethanol sorption capacity was approximately 50% higher for complex **2** in comparison to complex **1**, reaching 0.097 $cm^3/g$ (3.4 $C_2H_5OH$ molecules per $Cu_{10}$ unit, Figure S16) for compound **2** at $PP_S^{-1} = 1$. The quantity of sorbed alcohol substrate is comparable to the sorption capacity of other porous coordination polymers with the same substrates.[28]

Estimation of the $S_{BET}$ ($S_{BET}$ is the surface area calculated with the Brunauer-Emmett-Teller model[29]) from the initial parts of the methanol or ethanol sorption isotherms gave values between 24 and 50 $m^2/g$ for both **1** and **2**. These values exceed the surface accessible for $N_2$ sorption (less than 5 $m^2/g$, vide infra), so the interaction of compounds **1** and **2** with alcohols is not classical physical sorption, but rather some sort of host-guest interaction that involves weak binding of the alcohol molecules by the complexes.[11a,12] These weak interactions most likely involve hydrogen bonds between the alcohol molecules and the structural elements of **1** or **2** and their strongly bound water molecules. Coordination to copper by the alcohol molecules is considered less likely, as the water ligands appear to remain attached to the copper ions after activation.

The nonclassical alcohol sorption and desorption isotherms[29] of **1** and **2** imply that interaction of complexes **1** and **2** with these alcohols results in structural rearrangements, most likely associated with separation of the chains. The maximum sorption capacity is governed not by the total volume of voids as estimated from the X-ray structure determinations, but by the interplay between the energy of interaction of substrate with structural units of the coordination compound and the energy of interaction of the structural elements within the crystal lattice (in other words, between the force that separates the $Cu_5$ units and the force that holds them together).[30] Since the $N_2$ sorption experiments indicated that the desolvated samples of **1** and **2** contained no pores (note that $N_2$ suffusion without sorption at 77 K is not possible), different host-guest interaction energies and different crystal lattice energies may be the reason for the differences in the sorption capacities found for compounds **1** and **2** in methanol and ethanol sorption experiments.

Comparison of the structures of **1** and **1a** can be helpful for understanding the changes that can occur on interaction of desolvated **1** with substrates like alcohols. Direct information about the structures of the desolvated compound, and the structures of the complexes at certain $PP_S^{-1}$ values, cannot be obtained by X-ray single crystal analysis because such single crystals usually collapse upon desolvation (especially when it is associated with structural rearrangements, as in the case of **1** and **1a**). In the sense that compounds **1** and **1a** represent two possible combinations of building blocks, $[Cu_5(ahpha)_4]^{2+}$ and $m$-$C_8H_4O_4^{2-}$, which correspond to local free energy minima, they could to a certain extent be considered as models of frameworks that can exist at different stages of alcohol sorption or desorption.

The events involved in the changes of the framework during alcohol sorption may be similar to the structural changes that would transform framework **1** to **1a**. For instance, such a process would include: (i) disassociation of one carboxylic group of the coordinated *m*-phthalate ligand in **1**; (ii) breaking of axial Cu–O′ bonds that link the pentanuclear metallacrown units in the $Cu_{10}$ unit, thus increasing the distance between the mean planes of these metallacrowns; (iii) "shifting" of the pentanuclear metallacrown units within a $Cu_{10}$ unit that is accompanied by the formation of new Cu–O bonds (Cu5–O9′ in **1a**). These transformations are schematically represented by the arrows in Figure 11. The orientations of the metallacrown planes with respect to the crystal lattice (*a*, *b* and *c* axes) are similar in both **1** and **1a**, which further indicates some similarity between the crystal structures of these two compounds.

The methanol sorption isotherms for **1** and **2** show that the uptake of methanol significantly increases at a $PP_S^{-1}$ value of about 0.6. This raises the question, as to whether or not the opening of the channels in the crystal lattices of the sorbents due to their interaction with methanol molecules is cooperative. Noting that in the case of noncooperative sorption the relationship between sorption capacity and pressure should be linear, we examined $A/A_{max}$ vs. $PP_S^{-1}$ plots (where $A$ and $A_{max}$ are the sorbed amount of solvent at partial pressure $P$ and the maximum amount of sorbed solvent, respectively), while paying heed to the possibility of an increase in $dA/dP$ as $P$ approaches $P_S$ due to sorbate

 © 2011 Wiley-VCH Verlag GmbH & Co. KGaA, Weinheim 

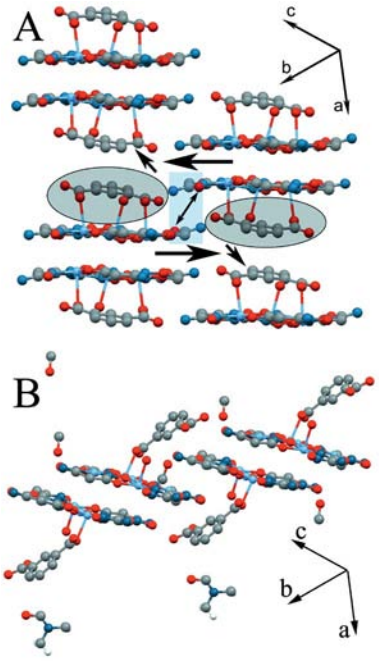


Figure 11. Comparison of crystal structures or **1** (A) and **1a** (B), also illustrated is a possible pathway for the transformations in desolvated **1** that can occur on alcohol sorption. Such a process may involve breaking of one bond between a coordinated *m*-phthalate ligand and a $Cu^{II}$ ion in each $[Cu_5(ahpha)_4]^{2+}$ unit, breaking of axial bond Cu3–O10′, which holds the $[Cu_5(ahpha)_4]^{2+}$ cations together within the $Cu_{10}$ unit, and "shifting" of the $[Cu_5(ahpha)_4]^{2+}$ units that is associated with the formation of dimers due to creation of new axial Cu5–O9′ bonds.

condensation (i.e. abrupt increase in the the isotherm at $PP_S^{-1} > 0.98$).

For ethanol sorption the values of $dA/dP$ oscillate around unity (Figure 12, Figure 13), and have high values only in the regions of very low and very high pressures, which may signal "classical" filling of some of the rigid micropores followed by interparticle condensation, respectively. In contrast, for methanol sorption the $d$A/$d$P curves for **1** and **2** have a clear maxima at $PP_S^{-1} \approx 0.85$, and this may be associated with a positive cooperative effect, namely, the sorption of the $(n-1)^{th}$ portion of methanol leading to structural changes that facilitate sorption of the $n^{th}$ portion.

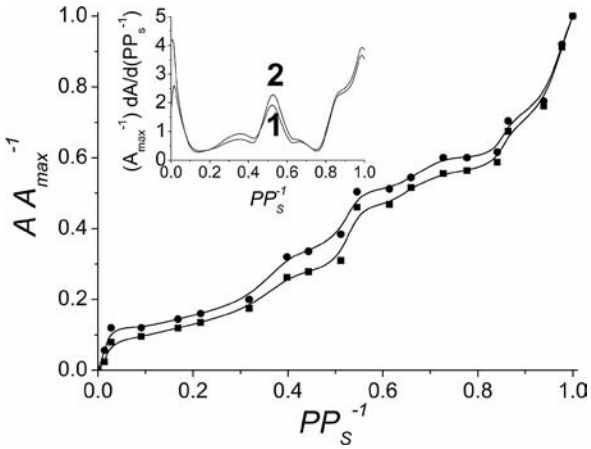


Figure 13. Ethanol sorption isotherms in reduced coordinates ($A{\cdot}A_{max}^{-1}$) and the derivatives of the reduced sorption $d(A{\cdot}A_{max}^{-1})/d(P{\cdot}P_s^{-1})$ (inset); (●) compound **1**, (■) compound **2**.

As in the case of alcohol sorption, compound **1** showed lower *n*-hexane uptake compared to complex **2** (Figure 14). Again, noticeable *n*-hexane sorption by compound **2** begins at a $PP_S^{-1}$ value of about 0.5, and at high pressures ($PP_S^{-1} > 0.8$) the sorption curve increases rapidly. The desorption curve does not follow the sorption one, and there is residual hexane that cannot be removed from the crystal at $10^{-2}$ Torr. Such behavior suggests the presence of nonpolar interactions between hexane and the lattice, which parallels the strong binding of ethanol by compound **2**. However, the size of the substrate molecule is also important in these host-guest interaction processes because a higher homologue of *n*-hexane (*n*-octane) showed only surface sorption, which is similar to the decrease in sorption capacity of 1 and 2 when exposed to ethanol vs. methanol.

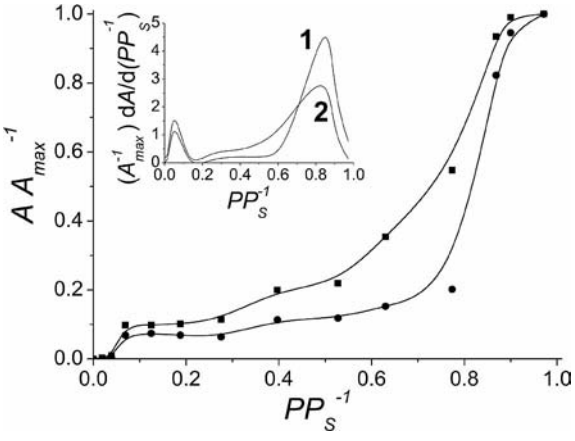


Figure 12. Methanol sorption isotherms in reduced coordinates ($A{\cdot}A_{max}^{-1}$) and the derivatives of the reduced sorption $d(A{\cdot}A_{max}^{-1})/d(P{\cdot}P_s^{-1})$ (inset); (●) compound **1**, (■) compound **2**.

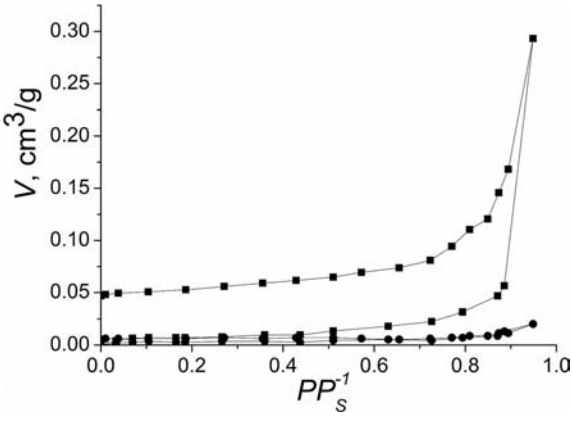


Figure 14. Hexane sorption and desorption isotherms for activated complexes **1** and **2** (20 °C); (●) compound **1**, (■) compound **2**.

 © 2011 Wiley-VCH Verlag GmbH & Co. KGaA, Weinheim 

## Conclusions

Linking of pentanuclear metallacrown cations $[Cu_5(ahpha)_4]^{2+}$ by *m*- or *p*-phthalates leads to the formation of supramolecular assemblies that possess cavities in their crystal structures that are capable of sorbing significant quantities of methanol and ethanol. The shapes of the sorption and desorption isotherms, as well as their hysteresis, indicate that sorption/desorption of these alcohols by complexes **1** and **2** is associated with structural rearrangements, which are probably induced by interactions between the substrates and structural elements of the complexes. To a certain extent, **1** and **1a** can be considered to represent two minima in the potential energy surface that includes the structures of the intermediates that can form during the sorption of alcohols by these complexes. To the best of our knowledge this paper presents the first study that gives some insight into the changes, which are usually called sorption-induced "structural rearrangements", that occur in supramolecular sorbents with non-rigid crystal structures in which the structural elements are not linked by covalent bonds.

The magnetic properties of these compounds are governed by exchange interactions within the pentanuclear metallacrown units. The differences in the exchange parameters between **1**, **2** and previously reported complexes containing the same cation $[Cu_5(ahpha)_4]^{2+}$, can be accounted for by distortions within the metallacrown unit.

## Experimental Section

**Materials and Measurements:** Commercially available reagents and solvents (Aldrich and Merck) were used without further purification. Elemental analyses (C, H, and N) were performed with a Carlo–Erba 1106 analyzer. IR spectra were measured with KBr pellets on a Perkin–Elmer Spectrum BX FTIR spectrometer in the range 400–4000 $cm^{-1}$. UV/Vis spectra were measured with the samples in DMF/water solutions and with a Cary 50 spectrophotometer. Thermogravimetric analysis (TGA) was performed with the samples in air with an MOM Q1500 instrument at a heating rate of 10 °C $min^{-1}$, and in the range 20–300 °C. Sorption measurements were performed with volumetric (for $N_2$ and $H_2$ at 77 K) and gravimetric (for methanol, ethanol, *n*-hexane, *n*-octane at 293 K) methods. For all sorption measurements samples were first activated at 130 °C in vacuo at $10^{-2}$ Torr. Each point on the sorption and desorption isotherms correspond to equilibrium conditions (constant sample weight at a given $PP_S^{-1}$ value). The volume of the crystal voids were calculated with the equation $V = m{\cdot}d$, where $m$ is the weight of sorbate at a given pressure, and $d$ is the density of sorbate at 293 K; this method gives a good approximation of the effective crystal volume.[29a] X-ray diffraction measurements were performed at 100 K on an Apex2 diffractometer with graphite monochromated Mo-$K_\alpha$ radiation of wavelength 0.71073 Å. Crystals of **1**, **1a** and **2** were taken directly from their reaction mixtures. Crystal data, data collection parameters and structure refinement details for complexes **1**, **1a** and **2** are given in Table 2. Temperature- and field-dependent magnetization measurements were carried out with a vibrating sample magnetometer from Quantum Design. Magnetization data were measured at temperatures ranging from 3 to 300 K in applied fields of 1000 and 5000 Oe. At the lowest temperature the magnetization of the samples was measured for fields up to 70 kOe. Susceptibility data were corrected for diamagnetism with Pascal's constants.[24]

The ligand $H_2$ahpha was synthesized by a method described previously.[20] The complex $[Cu_5(ahpha)_4](ClO_4)_2$ was prepared by a modified version of the procedure reported for $[Cu_5(ahpha)_4](NO_3)_2{\cdot}4H_2O$; specifically $Cu(ClO_4)_2{\cdot}6H_2O$ was used instead of copper(II) nitrate.[12,20]

Table 2. Single crystal data and structure refinement details for complexes **1**, **1a** and **2**.

| | **1** | **1a** | **2** |
|---|---|---|---|
| Empirical formula | $C_{20}H_{44}Cu_5N_{12}O_{26}$ | $C_{25}H_{41}Cu_5N_{13}O_{20}$ | $C_{40}H_{84}Cu_{10}N_{24}O_{50}$ |
| $M$ /g mol$^{-1}$ | 1186.42 | 1161.41 | 2336.81 |
| Crystal size /mm$^3$ | $0.30\times0.15\times0.02$ | $0.20\times0.14\times0.06$ | $0.28\times0.11\times0.03$ |
| Crystal system | triclinic | triclinic | monoclinic |
| Space group | $P\bar{1}$ | $P\bar{1}$ | $P2_1/c$ |
| $a$ /Å | 10.3219(15) | 8.580(5) | 16.6804(16) |
| $b$ /Å | 13.3076(19) | 14.150(7) | 19.6675(18) |
| $c$ /Å | 15.352(2) | 17.002(9) | 11.4711(11) |
| $\alpha$ /° | 67.301(2) | 66.385(2) | 90 |
| $\beta$ /° | 88.087(2) | 88.391(2) | 98.119(2) |
| $\gamma$ /° | 81.059(2) | 88.562(2) | 90 |
| Volume /Å$^3$ | 1921.0(5) | 1879.0(17) | 3725.5(6) |
| $Z$ | 2 | 2 | 2 |
| Range of data collection | $1.68° \le \theta \le 25.76°$ | $1.31° \le \theta \le 30.24°$ | $1.61° \le \theta \le 28.28°$ |
| $\rho_{calc}$ /g cm$^{-3}$ | 2.051 | 2.053 | 2.083 |
| $F(000)$ | 1202 | 1174 | 2364 |
| Absorption coefficient, $\mu$ /mm$^{-1}$ | 2.836 | 2.886 | 2.921 |
| $\lambda$(Mo-$K_\alpha$) /Å | 0.71073 | 0.71073 | 0.71073 |
| $T$ /K | 100(2) | 100(2) | 100(2) |
| Number of reflections | 16042 | 21178 | 37393 |
| Independent reflections | 7280 | 10731 | 9228 |
| Number of variables | 663 | 596 | 641 |
| $R_{int}$ | 0.0292 | 0.0445 | 0.0604 |
| Goodness-of-fit on $F^2$ | 1.047 | 1.083 | 1.040 |
| $R_1$ $[I>2\sigma(I)]$[a] | 0.0332 | 0.0547 | 0.0458 |
| $wR_2$ $[I>2\sigma(I)]$[b] | 0.0671 | 0.1130 | 0.0981 |

[a] $R_1 = \Sigma||F_o| - |F_c||/\Sigma|F_o|$. [b] $wR_2 = \{\Sigma[w(F_o^2 - F_c^2)^2]/\Sigma[w\,(F_o^2)^2]\}^{1/2}$.

 © 2011 Wiley-VCH Verlag GmbH & Co. KGaA, Weinheim 

***Caution:*** *Perchlorate salts are potentially explosive and should be handled with care and in small quantities.*

**$[Cu_5(ahpha)_4](ClO_4)_2·4H_2O$:** $Cu(ClO_4)_2·6H_2O$ (2.79 g, 7.519 mmol) was dissolved in water (15 mL) and added to a stirred solution of $H_2$ahpha (1 g, 7.52 mmol) in water (35 mL). After two days, finely divided prismatic green crystals were obtained (1.54 g, 92% yield). $C_{12}H_{28}Cl_2Cu_5N_{12}O_{24}$ (1113.06): calcd. C 12.9, H 2.51, N 15.1; found C 12.5, H 2.56, N 14.8. The identity of the compound was confirmed by single crystal X-ray structure determination (Supporting Information, Figures S20 and S21).

**$[Cu_5(ahpha)_4(m\text{-}C_8H_4O_4)(H_2O)]·9H_2O$ (1):** $[Cu_5(ahpha)_4](ClO_4)_2·4H_2O$ (20 mg, 0.019 mmol) was dissolved in DMF (1.5 mL) and added to a stirred solution of 1,3-$C_8H_4O_4Na_2$ (8 mg, 0.04 mmol, 50% excess) in water (3 mL). After two days prismatic green crystals were obtained (19 mg, 84% yield). $C_{20}H_{36}Cu_5N_{12}O_{22}$ (1114.30): calcd. C 21.4, H 3.22, N 14.9; found C 21.3, H 2.74, N 14.4. Wet crystals were used for X-ray diffraction.

**$[Cu_5(ahpha)_4(m\text{-}C_8H_4O_4)(H_2O)]·2MeOH·DMF$ (1a):** $[Cu_5(ahpha)_4](ClO_4)_2·4H_2O$ (20 mg, 0.019 mmol) was dissolved in DMF (1.5 mL) and added to a stirred solution of 1,3-$C_8H_6O_4$ (7 mg, 0.04 mmol, 50% excess) in methanol (3 mL). Slow evaporation of this solution resulted in the formation of green crystals (15 mg, 68% yield). $C_{25}H_{41}Cu_5N_{13}O_{20}$ (1161.41): calcd. C 25.85, H 3.56, N 15.68; found C 25.63, H 3.92, N 15.87.

**$[Cu_5(ahpha)_4(p\text{-}C_8H_4O_4)(H_2O)_2]_2·14H_2O$ (2):** $[Cu_5(ahpha)_4](ClO_4)_2·4H_2O$ (20 mg, 0.019 mmol) was dissolved in DMF (1.5 mL) and added to a stirred solution of 1,4-$C_8H_4O_4Na_2$ (8 mg, 0.04 mmol, 50% excess) in water (3 mL). After two days prismatic green crystals were obtained (18 mg, 81% yield). $C_{40}H_{84}Cu_{10}N_{24}O_{50}$ (2336.81): calcd. C 20.6, H 3.63, N 14.4; found C 20.7, H 3.62, N 14.3.

**Supporting Information** (see footnote on the first page of this article): Additional figures illustrating the crystal structures of compounds **1**, **1a** and **2**, data regarding the X-ray crystal structure determination of $[Cu_5(ahpha)_4](ClO_4)_2·2.87DMF$, IR spectra for compounds **1**, **1a** and **2**, UV/Vis spectra for compounds **1** and **2**, and TG curves for **1** and **2**.

CCDC-826385 (for **1**), -826386 (for **1a**), -826387 {for $[Cu_5(ahpha)_4](ClO_4)_2·4H_2O$} and -826388 (for **2**) contain the supplementary crystallographic data for this paper. These data can be obtained free of charge from The Cambridge Crystallographic Data Centre via www.ccdc.cam.ac.uk/data_request/cif.

## Acknowledgments

We thank Prof. V. G. Ilyin, V. V. Tsyrina and V. N. Solomakha for their kind assistance with sorption measurements. A. W. A. thanks Drexel University for support. S. V. K. thanks the National Academy of Sciences of Ukraine for support (through joint grant number 7/2P-2011 of the NAS of Ukraine and the Russian Foundation for Basic Research). The X-ray diffractometer was funded by National Science Foundation (NSF), grant number 0087210, Ohio Board of Regents, grant number CAP-491, and by Youngstown State University.

[1] a) A. Mallick, S. Saha, P. Pachfule, S. Roy, R. Banerjee, *J. Mater. Chem.* **2010**, *20*, 9073–9080; b) S. K. Ghosh, S. Bureekaew, S. Kitagawa, *Angew. Chem.* **2008**, *120*, 3451; *Angew. Chem. Int. Ed.* **2008**, *47*, 3403–3406; c) X. Wang, L. Liu, A. J. Jacobson, *Angew. Chem.* **2006**, *118*, 6649–6653; *Angew. Chem. Int. Ed.* **2006**, *45*, 6499–6503; d) J. Milon, M.-C. Daniel, A. Kaiba, P. Guionneau, S. Brandès, J.-P. Sutter, *J. Am. Chem. Soc.* **2007**, *129*, 13872–13878; e) M. A. Nadeem, A. W. Thornton, M. R. Hill, J. A. Stride, *Dalton Trans.* **2011**, *40*, 3398–3401; f) D. Zhao, D. Yuan, R. Krishna, J. M. van Baten, H.-C. Zhou, *Chem. Commun.* **2010**, *46*, 7352–7354; g) J. Y. Lu, A. M. Babb, *Chem. Commun.* **2002**, 1340–1341.

[2] a) B. Chen, C. Liang, J. Yang, D. S. Contreras, Y. L. Clancy, E. B. Lobkovsky, O. M. Yaghi, S. Dai, *Angew. Chem.* **2006**, *118*, 1418–1421; *Angew. Chem. Int. Ed.* **2006**, *45*, 1390–1393; b) L. Alaerts, C. E. A. Kirschhock, M. Maes, M. A. van der Veen, V. Finsy, A. Depla, J. A. Martens, G. V. Baron, P. A. Jacobs, J. F. M. Denayer, D. E. De Vos, *Angew. Chem.* **2007**, *119*, 4371–4375; *Angew. Chem. Int. Ed.* **2007**, *46*, 4293–4297.

[3] a) S. Hasegawa, S. Horike, R. Matsuda, S. Furukawa, K. Mochizuki, Y. Kinoshita, S. Kitagawa, *J. Am. Chem. Soc.* **2007**, *129*, 2607–2614; b) D. N. Dybtsev, A. L. Nuzhdin, H. Chun, K. P. Bryliakov, E. P. Talsi, V. P. Fedin, K. Kim, *Angew. Chem.* **2006**, *118*, 930–934; *Angew. Chem. Int. Ed.* **2006**, *45*, 916–920; c) J. W. Han, C. L. Hill, *J. Am. Chem. Soc.* **2007**, *129*, 15094–15095; d) T. Ladrak, S. Smulders, O. Roubeau, S. J. Teat, P. Gamez, J. Reedijk, *Eur. J. Inorg. Chem.* **2010**, 3804–3812; e) K. Ohara, Y. Inokuma, M. Fujita, *Angew. Chem. Int. Ed.* **2010**, *49*, 5507–5509.

[4] a) W. Kaneko, M. Ohba, S. Kitagawa, *J. Am. Chem. Soc.* **2007**, *129*, 13706–13712; b) A. S. Lytvynenko, S. V. Kolotilov, O. Cador, K. S. Gavrilenko, S. Golhen, L. Ouahab, V. V. Pavlishchuk, *Dalton Trans.* **2009**, 3503–3509; c) N. Yanai, W. Kaneko, K. Yoneda, M. Ohba, S. Kitagawa, *J. Am. Chem. Soc.* **2007**, *129*, 3496–3407.

[5] a) B. Chen, Y. Yang, F. Zapata, G. Lin, G. Qian, E. B. Lobkovsky, *Adv. Mater.* **2007**, *19*, 1693–1696; b) C. A. Bauer, T. V. Timofeeva, T. B. Settersten, B. D. Patterson, V. H. Liu, B. A. Simmons, M. D. Allendorf, *J. Am. Chem. Soc.* **2007**, *129*, 7136–7144; c) L. G. Beauvais, M. P. Shores, J. R. Long, *J. Am. Chem. Soc.* **2000**, *122*, 2763–2772.

[6] a) M. P. Suh, Y. E. Cheon, E. Y. Lee, *Coord. Chem. Rev.* **2008**, *252*, 1007–1026; b) R. J. Kuppler, D. J. Timmons, Q. R. Fang, J.-R. Li, T. A. Makal, M. D. Young, D. Yuan, D. Zhao, W. Zhuang, H.-C. Zhou, *Coord. Chem. Rev.* **2009**, *253*, 3042–3066; c) S. Henke, R. Schmid, J.-D. Grunwaldt, R. A. Fischer, *Chem. Eur. J.* **2010**, *16*, 14296–14306; d) J.-J. Jiang, L. Li, M.-H. Lan, M. Pan, A. Eichhçfer, D. Fenske, C.-Y. Su, *Chem. Eur. J.* **2010**, *16*, 1841–1848; e) A. Demessence, J. R. Long, *Chem. Eur. J.* **2010**, *16*, 5902–5908.

[7] a) E. Y. Lee, M. P. Suh, *Angew. Chem.* **2004**, *116*, 2858–2861; *Angew. Chem. Int. Ed.* **2004**, *43*, 2798–2801; b) S. Horike, S. Hasegawa, D. Tanaka, M. Higuchi, S. Kitagawa, *Chem. Commun.* **2008**, 4436–4438; c) M. Eddaoudi, D. B. Moler, H. Li, B. Chen, T. M. Reineke, M. O'Keeffe, O. M. Yaghi, *Acc. Chem. Res.* **2001**, *34*, 319–330.

[8] a) S. Kitagawa, K. Uemura, *Chem. Soc. Rev.* **2005**, *34*, 109–119; b) K. Uemura, S. Kitagawa, M. Kondo, K. Fukui, R. Kitaura, H.-C. Chang, T. Mizutani, *Chem. Eur. J.* **2002**, *8*, 3586–3600; c) S. Bureekaew, S. Shimomura, S. Kitagawa, *Sci. Technol. Adv. Mater.* **2008**, *9*, 014108.

[9] a) G. Férey, C. Serre, *Chem. Soc. Rev.* **2009**, *38*, 1380–1399.

[10] J. A. R. Navarro, E. Barea, A. Rodríguez-Diéguez, J. M. Salas, C. O. Ania, J. B. Parra, N. Masciocchi, S. Galli, A. Sironi, *J. Am. Chem. Soc.* **2008**, *130*, 3978–3984.

[11] a) S. Uchida, M. Hashimoto, N. Mizuno, *Angew. Chem.* **2002**, *114*, 2938–2941; *Angew. Chem. Int. Ed.* **2002**, *41*, 2814–2817; b) S. Uchida, N. Mizuno, *Coord. Chem. Rev.* **2007**, *251*, 2537–2546.

[12] A. V. Pavlishchuk, S. V. Kolotilov, M. Zeller, L. K. Thompson, I. O. Fritsky, A. W. Addison, A. D. Hunter, *Eur. J. Inorg. Chem.* **2010**, 4851–4858.

[13] M. Edgar, R. Mitchell, A. M. Z. Slawin, P. Lightfoot, P. A. Wright, *Chem. Eur. J.* **2001**, *7*, 5168–5175.

[14] a) C. M. Zaleski, E. C. Depperman, J. W. Kampf, M. L. Kirk, V. L. Pecoraro, *Angew. Chem.* **2004**, *116*, 4002–4004; *Angew.*

 © 2011 Wiley-VCH Verlag GmbH & Co. KGaA, Weinheim 

*Chem. Int. Ed.* **2004**, *43*, 3912–3914; b) C. M. Zaleski, E. C. Depperman, J. W. Kampf, M. L. Kirk, V. L. Pecoraro, *Inorg. Chem.* **2006**, *45*, 10022–10024; c) C. M. Zaleski, J. W. Kampf, T. Mallah, M. L. Kirk, V. L. Pecoraro, *Inorg. Chem.* **2007**, *46*, 1954–1956; d) B. R. Gibney, D. P. Kessissoglou, J. W. Kampf, V. L. Pecoraro, *Inorg. Chem.* **1994**, *33*, 4840–4849.

[15] a) T. Afrati, C. Dendrinou-Samara, C. Raptopoulou, A. Terzis, V. Tangoulis, A. Tsipis, D. P. Kessissoglou, *Inorg. Chem.* **2008**, *47*, 7545–7555; b) A. J. Stemmler, J. W. Kampf, M. L. Kirk, B. H. Atasi, V. L. Pecoraro, *Inorg. Chem.* **1999**, *38*, 2807–2817; c) T. Afrati, C. Dendrinou-Samara, C. Raptopoulou, A. Terzis, V. Tangoulis, D. P. Kessissoglou, *Dalton Trans.* **2007**, 5156–5164; d) G. Mezei, C. M. Zaleski, V. L. Pecoraro, *Chem. Rev.* **2007**, *107*, 4933–5003.

[16] a) F.-P. Xiao, L.-F. Jin, G.-Z. Cheng, Z.-P. Ji, *Polyhedron* **2007**, *26*, 2695–2702; b) M. Tegoni, F. Dallavalle, M. A. Santos, *J. Inorg. Biochem.* **2004**, *98*, 209–218; c) C. Dendrinou-Samara, A. N. Papadopoulos, D. A. Malamatari, A. Tarushi, C. P. Raptopoulou, A. Terzis, E. Samaras, D. P. Kessissoglou, *J. Inorg. Biochem.* **2005**, *99*, 864–875.

[17] a) J. J. Bodwin, A. D. Cutland, R. G. Malkani, V. L. Pecoraro, *Coord. Chem. Rev.* **2001**, *216–217*, 489–512; b) B. R. Gibney, H. Wang, J. W. Kampf, V. L. Pecoraro, *Inorg. Chem.* **1996**, *35*, 6184–6193; c) D. P. Kessissoglou, J. J. Bodwin, J. Kampf, C. Dendrinou-Samara, V. L. Pecoraro, *Inorg. Chim. Acta* **2002**, *331*, 73–80.

[18] a) A. D. Cutland, J. A. Halfen, J. W. Kampf, V. L. Pecoraro, *J. Am. Chem. Soc.* **2001**, *123*, 6211–6212; b) C.-S. Lim, J. W. Kampf, V. L. Pecoraro, *Inorg. Chem.* **2009**, *48*, 5224–5233; c) C.-S. Lim, A. C. Van Noord, J. W. Kampf, V. L. Pecoraro, *Eur. J. Inorg. Chem.* **2007**, 1347–1350.

[19] a) J. J. Bodwin, V. L. Pecoraro, *Inorg. Chem.* **2000**, *39*, 3434–3435; b) C.-S. Lim, J. Jankolovits, J. W. Kampf, V. L. Pecoraro, *Chem. Asian J.* **2010**, *5*, 46–49.

[20] Y. Song, J.-C. Liu, Y.-J. Liu, D.-R. Zhu, J.-Z. Zhuang, X.-Z. You, *Inorg. Chim. Acta* **2000**, *305*, 135–142.

[21] A. W. Addison, T. N. Rao, J. Reedijk, J. van Rijn, G. C. Verschoor, *J. Chem. Soc., Dalton Trans.* **1984**, 1349–1356.

[22] H. Yokoi, A. W. Addison, *Inorg. Chem.* **1977**, *16*, 1341–1349.

[23] a) A. L. Spek, *Acta Crystallogr., Sect. A* **1990**, *46*, C34; b) A. L. Spek, *PLATON – A Multipurpose Crystallographic Tool*, Utrecht University, The Netherlands, **2006**.

[24] O. Kahn in *Molecular Magnetism*, VCH Publishers Inc., Weinheim, **1993**.

[25] The measure of the deviation of the fit is $R^2 = \Sigma[(\chi_M T)_{obs.} - (\chi_M T)_{calcd.}]^2/[\Sigma(\chi_M T)_{obs.}{}^2]$.

[26] a) D. Tanaka, K. Nakagawa, M. Higuchi, S. Horike, Y. Kubota, T. C. Kobayashi, M. Takata, S. Kitagawa, *Angew. Chem.* **2008**, *120*, 3978–3982; *Angew. Chem. Int. Ed.* **2008**, *47*, 3914–3918; b) R. Kitaura, K. Seki, G. Akiyama, S. Kitagawa, *Angew. Chem.* **2003**, *115*, 444–447; *Angew. Chem. Int. Ed.* **2003**, *42*, 428–431; c) H. Chun, J. Seo, *Inorg. Chem.* **2009**, *48*, 9980–9982.

[27] a) P. Kanoo, K. L. Gurunatha, T. K. Maji, *J. Mater. Chem.* **2010**, *20*, 1322–1331; b) A. J. Fletcher, K. M. Thomas, M. J. Rosseinsky, *J. Solid State Chem.* **2005**, *178*, 2491–2510; c) S. K. Ghosh, S. Bureekaew, S. Kitagawa, *Angew. Chem.* **2008**, *120*, 3451–3454; *Angew. Chem. Int. Ed.* **2008**, *47*, 3403–3406.

[28] T. M. Reineke, M. Eddaoudi, M. O'Keeffe, O. M. Yaghi, *Angew. Chem.* **1999**, *111*, 2712–2716; *Angew. Chem. Int. Ed.* **1999**, *38*, 2590–2594.

[29] a) K. S. W. Sing, D. H. Everett, R. A. W. Haul, L. Moscou, R. A. Pierotti, J. Rouquerol, T. Siemieniewska, *Pure Appl. Chem.* **1985**, *57*, 603–619; b) S. J. Gregg, K. S. W. Sing in *Adsorption, Surface Area and Porosity*, 2nd ed., Academic Press, London, **1982**, pp. 4.

[30] S. V. Kolotilov, N. N. Stepanenko, Z. V. Chernenko, A. V. Shvets, *Theor. Exp. Chem.* **2008**, *44*, 60–65.

Received: July 28, 2011
Published Online: September 26, 2011

 © 2011 Wiley-VCH Verlag GmbH & Co. KGaA, Weinheim 